Check for updates

IWA PUBLISHING

Integrated assessment of flood and drought hazards for current and future climate in a tributary of the Mekong river basin

Jessica Penny [IWA] [iD][a,*], Dibesh Khadka [iD][b], Mukand Babel [iD][a,b], Priscila Alves[c], Slobodan Djordjević [IWA] [iD][a,d], Albert S. Chen [IWA][a] and Ho Huu Loc[e]

[a] Centre for Water Systems, College of Engineering, Mathematics, and Physical Sciences, University of Exeter, Exeter, UK
[b] Water Engineering and Management, School of Engineering and Technology, Asian Institute of Technology, Pathum Thani, Bangkok, Thailand
[c] Stormwater Infrastructure Resilience and Justice Lab, School of Architecture, Planning and Preservation, University of Maryland, USA
[d] Faculty of Civil Engineering, University of Belgrade, Belgrade 11000, Serbia
[e] Water Systems and Global Change Group, Wageningen University, The Netherlands
*Corresponding author. E-mail: jp606@exeter.ac.uk

[iD] JP, 0000-0001-8748-472X; DK, 0000-0002-5703-5306; MB, 0000-0003-4203-0059; SD, 0000-0003-1682-1383

ABSTRACT

Projecting floods and droughts characteristics under climate change is important to formulate an integrative management plan and enhance resiliency of society. However, studies that provide the integration of floods-drought hazards are scarce within literature. This study assessed flood and drought hazards separately and together for future climate in the Mun River basin, a tributary of the Mekong river. A non-modelling and multi-variate approach was used to assess flood and drought hazard respectively. Climate model ensemble suggests that the area under 'high' and 'very high' drought hazard level will increase from 27% and 4% during baseline period (1981–2010) to 43% and 37%, respectively, during near-future period (2021–2050). Similarly, an increase in 'high' and 'very high' flood hazard from 11% and 22% during baseline period to 16% and 24% during near-future period is projected. When both hazards are considered together, the total hazard is projected to increase by 155% in the near-future period. 76% of the catchment during the near future period will have combined hazard level from 'medium' to 'very high' compared to the 30% during the baseline period. The research presents a grim outlook on for the basin, with the area at risk from both hydro-meteorological hazards.

Key words: climate change, hydro-meteorological hazards, multi criteria decision analysis, geographical information systems, multi-variate approach, Mun River basin

HIGHLIGHTS

- Individual and combined flood and drought hazard assessment for the near-future period.
- Non-modelling approach for flood and a multi-variate approach for drought hazards used.
- Area under high and very high drought hazards up from 30 to 80% in the near future.
- Area under high and very high flood hazards up from 33 to 40% in the near future.
- Area under the combined hazard projected to increase by 155% across the catchment.

1. INTRODUCTION

Hydro-meteorological extremes, either an acute lack of water or excess of it, are characterized by spatial–temporal variability and manifest as droughts or floods , respectively. They have the potential to cause severe damage to the environment (Masud *et al.* 2015), have a significant effect on the hydrology and water resources of watersheds (Aalijahan *et al.* 2021), and cause socio-economic impacts (Marcos-Garcia *et al.* 2017). Between 2005 and 2014, 83% of the recorded disasters, 39% of the recorded human deaths and 70% of the documented damages were linked to weather, water and climate (WMO 2018), respectively. With climate change, hydro-meteorological hazards are likely to be more frequent and severe, and influence a greater area. A warmer climate will intensify the hydrological cycle, resulting in the spatial and temporal redistribution of global water resources (Chen & Sun 2017).

With almost one billion people living in flood-prone areas (Kittipongvises *et al.* 2020), flooding is one of the most destructive natural hazards in the world, affecting 45% of the global population (Hammond *et al.* 2014; Kittipongvises *et al.* 2020) and causing billions of dollars of damage each year (Davenport *et al.* 2021). Several studies have shown that precipitation extremes will increase in the frequency and magnitude in the future (Zhu 2013; Rudra *et al.* 2015; Burke & Stott 2017; Ohba & Sugimoto 2019). An increase in the extreme precipitation will be manifested as an increase in the flood risk.

Problems caused by flooding are increasingly exacerbated by increased water vapour in the atmosphere (Morita 2011; Aalijahan *et al.* 2023), a higher frequency of intense rainfall events (Chitwatkulsiri *et al.* 2021) and changes in land use, increasing surface runoff, resulting in greater flood extents and depths (Khan *et al.* 2018; Penny *et al.* 2023). In particular, South Asia is one of the most flood-prone regions in the world due to its natural geography (Shah *et al.* 2020).

On par with flooding, between the 2008 and 2018 period, global drought resulted in economic losses of about 8.42 billion USD (CRED 2018). A study by Lesk *et al.* (2016) showed that between 1964 and 2007, drought resulted in an estimated loss of 1,820 million metric tons of cereal globally. There are several types of droughts: meteorological, agricultural, hydrological, groundwater, ecological, socio-economical, etc. (Mishra & Singh 2010; Zargar *et al.* 2011; Crausbay *et al.* 2018). Under climate change, global agricultural droughts are projected to increase (Zhao & Dai 2017), several studies in Asian river basins have similar conclusions (Nam *et al.* 2015; Lu *et al.* 2016; Li *et al.* 2017; Kwon & Sung 2019).

Floods and droughts are common natural hazards with dire consequences in Thailand. The probability of drought in any given year is 0.45 for Thailand, the highest among Asia–Pacific countries (Pandey *et al.* 2007). While the droughts of 2004–2005 caused an estimated damage of about 220 million USD (Wichitarapongsakun *et al.* 2016), the devastating drought of 2015–2017 resulted in a damage of 3,300 million USD (EM-DAT 2019). On the other hand, flooding is also a serious issue in Thailand, experiencing 69 major floods since 1985 (Singkran 2017). The historic flooding of 2011–2012 affected 16 million people in 64 provinces out of 77 and caused a damage of about 45.7 billion USD (DDPM 2015). The World Bank estimated it to be the fourth most costly natural disaster in the world from 1995 to 2011 (Kittipongvises *et al.* 2020). Other studies in Thailand have shown that extreme precipitation is likely to increase in the future (Singhrattna *et al.* 2012; Komori *et al.* 2018; Igarashi *et al.* 2019), consequently increasing the flood hazard.

There have been many methods that examine flood and drought hazards: hydrologic–hydraulic modelling approach (Vojinovic *et al.* 2016; Jacob *et al.* 2020), hydrographs (Samu & Akıntuğ 2020), frequency ratio (Kongmuang *et al.* 2020), Flood and Drought Disasters (FDD) index (Guan *et al.* 2021), Normalized Difference Vegetation Index (NDVI) and LSWI (Chandrasekar *et al.* 2010; Navarathinam *et al.* 2015) and the modified Mann–Kendall (MMK) (Gemmer *et al.* 2008; Zhang *et al.* 2015). However, lately Geographical Information Systems (GIS) techniques are increasingly used in flood hazard, with the Standardized Precipitation Index (SPI) and Standardized Precipitation Index (SPEI) used in drought assessments (Nawai *et al.* 2015; Prabnakorn 2020; Prabnakorn *et al.* 2016, 2021; Shao & Kam 2020). MCDA-GIS is a combination of GIS with multi-criteria decision analysis (MCDA). GIS-based MCDA is a method increasingly used over the past two decades for flood risk and hazard assessment (Tang *et al.* 2018; Shadmehri Toosi *et al.* 2019, 2020; Kittipongvises *et al.* 2020) that provides a simple, effective and accurate means to investigate spatial distributions and characteristics using basic GIS analysis and mapping (Paquette & Lowry 2012; Samanta *et al.* 2016; Shadmehri Toosi *et al.* 2020). It is an especially useful method in areas where there are limited data (Shadmehri Toosi *et al.* 2020). MCDA-GIS provides more flexibility for decision makers to evaluate factors that cause flooding (Nigusse & Adhanom 2019), providing significant advantages over different methods in overcoming decision-making difficulties (Vavatsikos *et al.* 2019).

Modelling multiple climate hazards together is rarely done. However, Ming *et al.* (2015) provided a quantitative approach of multi-hazard risk assessment to assess crop losses caused by high winds and flooding. Typically, droughts and flooding are treated independently due to challenges, associated with their subjective nature and their coupled dynamics. Recently, Brunner *et al.* (2021) have suggested that droughts and floods should be studied in a joint framework to help learn about fast event transitions. For example, Forzieri *et al.* (2016) modelled multiple hazards (flooding, drought, heatwaves) over Europe using the Overall Exposure Index (OEI), which works under the assumption that hazards are mutually non-exclusive and the Change Exposure Index (CEI), which expresses the number of hazards at a given baseline period. Tabari *et al.* (2021) agrees with Forzieri *et al.* (2016), stating that few studies and combined and projected flood and drought risk owing to large uncertainties, non-linerities and complex spatial-temporal dynamics. Tabari *et al.* (2021) also develops a global framework to encapsulate changes in flood and drought hazards using Extreme Value Distribution (GEV), SPEI and SPI. Nevertheless, both the above studies failed to combine the hazards within one map/entity. More recently, Yang *et al.* (2023) have combined

the drought and flood status with crop yield through a correlation approach using SPEI to identify the risk from each hazard through both linear and probabilistic analyses. The study concluded that there were uncertainties within the models used and the level of risk classification.

To conclude, floods and droughts are significant disasters with severe implications to the society. It is important to understand and quantify them, especially with the ever disheartening climate change outlook, so that measures can be designed to mitigate them. Consequently, this study considers the joint spatial patterns of the flood and drought hazards in the Mun River basin, Thailand, for present and future climate scenarios. While previous studies have looked at either flood or drought hazard separately, this study presents its novelty by providing a non-modelling approach to joint hazard analysis considering both flood and drought. The methodology, using MCDA-GIS, is applicable to other studies as it is not limited by detailed data needs as found with hydrological/hydraulic modelling. The study will be useful to identify the areas where both single flood and drought hazards are located, as well as areas at risk from combined hazards, which could be a basis for implementing measures to improve resilience and reduce the associated risk in the future against both hydro-meteorological extremes commonly occurring in basins across the globe.

2. STUDY AREA AND METHODOLOGY

2.1. Study area

The Mun River basin (as shown in Figure 1) is the largest basin in northeast Thailand and has a catchment area of about 53,800 km^2. It is one of the major tributaries of the Mekong river. As part of the Korat plateau, the elevation varies between 64 m in the central region to 1,351 m in the south-west area (Khadka et al. 2022). The basin comprises four provinces, namely,
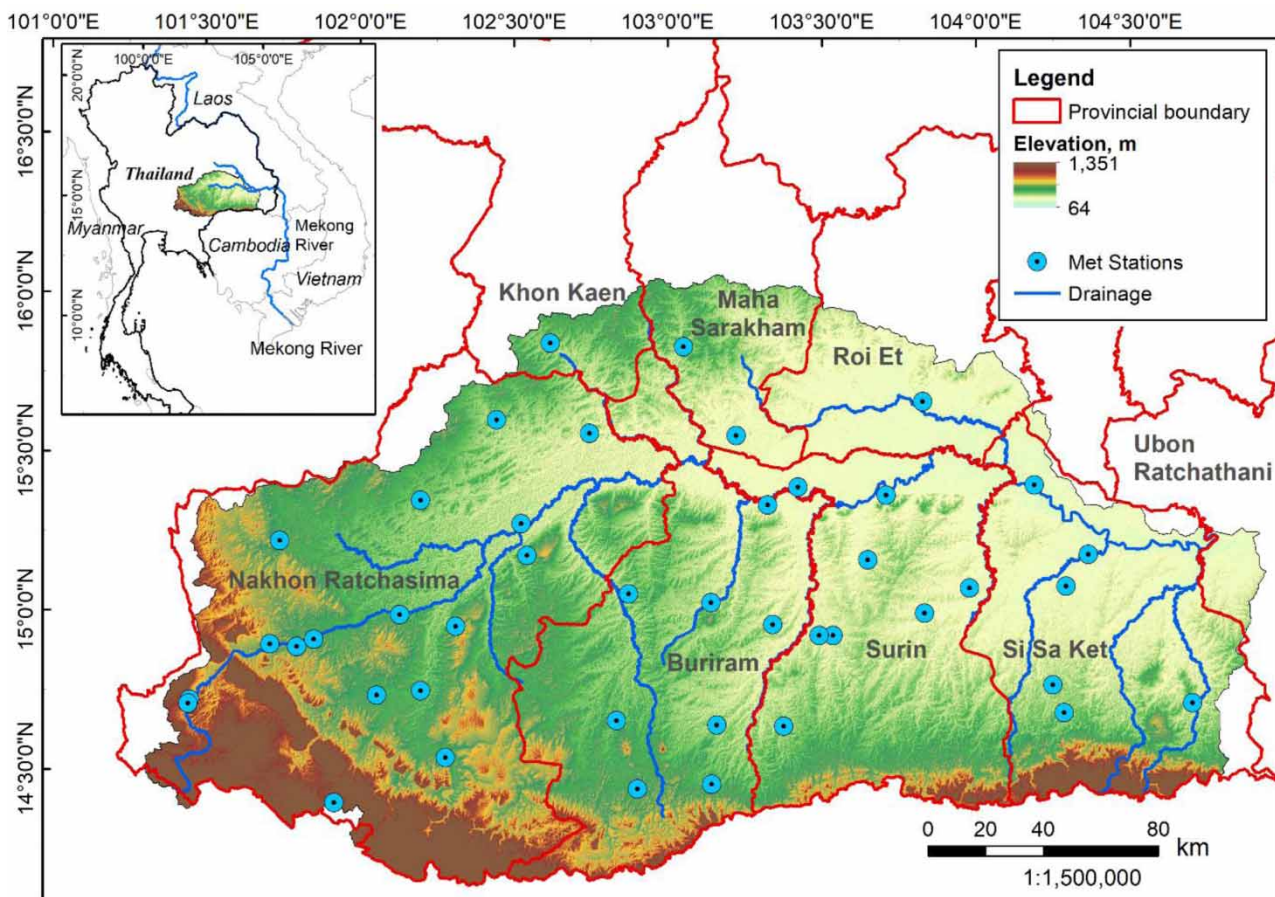

Figure 1 | The study area of the Mun River basin, located in northeast Thailand, hydrological and provincial boundaries.

Nakhon Ratchasima, Buriram, Surin and Si Sa Ket, and partially another four (Roi Et, Maha Sarakham, Khon Khen and Ubon Ratchathani). Even though the basin is one of the most drought prone regions in the country (Khadka et al. 2021), it is also an important agricultural region (Penny et al. 2021) of the country with rice cultivation occupying approximately 75% of the agricultural land and 55% of the basin's total area (Penny et al. 2021; Prabnakorn et al. 2021). The climate of the basin is primarily governed by the south-west monsoonal system, which brings heavy rainfall during mid-May to mid-October (providing about 80% of the annual rainfall). Consequently, the basin is prone to flooding especially within these months (Prabnakorn et al. 2019). However, the winter monsoonal system (December to February) is relatively dry, with the summer months extending from March to May. As the basin regularly experiences considerable problems caused by floods in the wet season and droughts in the dry season (Prabnakorn 2020; Prabnakorn et al. 2021), it makes an excellent case study.

2.2. Topographic and land use (LU) dataset

Data sources and GIS tools used to create the driving map can be observed in Table 1. Land use classes were identified according to the land use maps supplied by the Land Development Department (LDD) of Thailand and were the ones identified by Penny et al. (2021) paddy fields, field crops, perennials and orchards, other agriculture, forest, water bodies, marsh and swamp, urban and miscellaneous. From land use data using the 'Distance tool', drainage density could also be calculated. Soil data were classified according to the Harmonized World Soil Database, a global soil database framed within a GIS, which contains up-to-date information on world soil resources, classification range from combinations of clay, loam and sand. A slope map was created using the surface toolbox within ArcMap 10.6.1 (ESRI) and an elevation map provided by ALOS-JAXA.

2.3. Observed climatic data

The study utilizes the gridded rainfall and temperature dataset prepared by Khadka et al. (2022). The observed rainfall data from 43 stations (acquired from Thai Meteorological Department) were spatially interpolated to 0.25-degree grids using the inverse distance weighting (IDW) method. The maximum and minimum temperature datasets from the Climate Prediction Center (CPC) Global land surface air temperature analysis (Fan & van den Dool 2008) were used after comparison with other data products to ensure accuracy and consistency.

Spatially, both maximum and minimum temperatures show very small variations within the study basin (<1.0 °C); however, considerable spatial variation in the rainfall is observed as it gradually increases from the west towards the east (Figure 2). The Nakhon Ratchasima province in the west receives the least rainfall (about 800 mm/year), while the Si Sa Ket province in the east receives the most rainfall (about 1,600 mm/year).

2.4. Future climate projection dataset

Near-future (2021–2050) climate, projected by Khadka et al. (2022), was used in this study. The climate projection (rainfall and temperatures) is based on eight climate models participating in HighResMIPs (Haarsma et al. 2016) of CMIP6 (Table 2). The study has assessed the changes in the climate for the near-future (2021–2050) with respect to the baseline period of

Table 1 | Details of the data type and sources used within flood hazard analysis

| Data type	Observation period	Spatial resolution	Organization source	GIS tools used
Land use of northeast Thailand	2016	100 m	Land Development Department (LDD)	Reclass – Reclassify
Drainage density (distance from river)		100 m		Data Management Tool – mosaic to new raster distance – Euclidean Distance
Soil data – lithology type	2008	100 m	Mekong river Commission (MRC)	Reclass – Reclassify
Topographic map – elevation and slope	2019	30 m	ALOS – JAXA	Reclass – Reclassify The Surface Tool – Slope
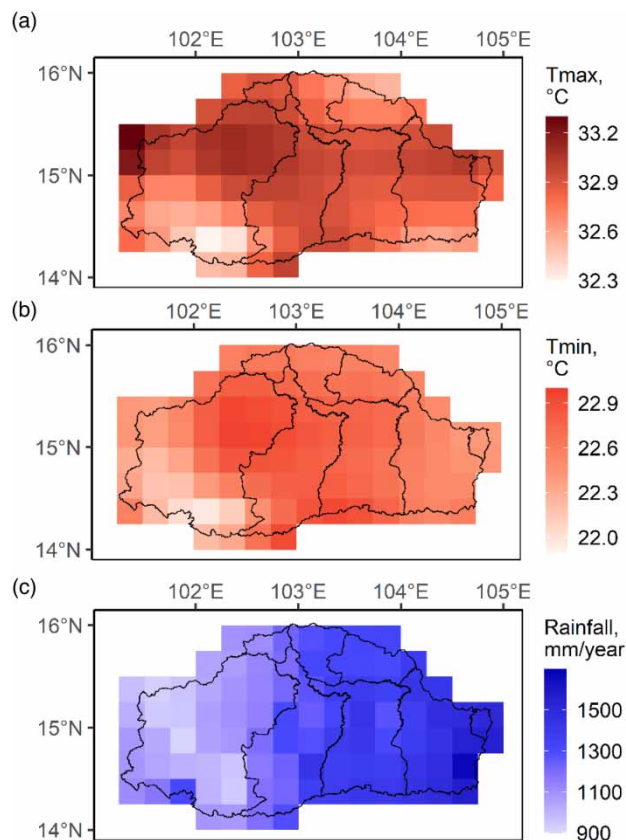
Figure 2 | Observed annual (a) maximum temperature, (b) minimum temperature, and (c) rainfall in the study area for 1981–2010 period.

Table 2 | Details of climate models used for the near-future climate in the Mun River basin (Khadka *et al.* 2022)

S.N.	Model designation	Modelling group	Atmospheric resolution (lat × lon)	Number of vertical levels	Ensemble member
1.	CNRM-CM6-1	Centre National de Recherches Meteorologiques (CNRM)/ Centre Europeen de Recherche et Formation Avancees en Calcul Scientifique	$1.4° \times 1.4°$	91	r1i1p1f2
2.	CNRM-CM6-1-HR	Centre National de Recherches Meteorologiques (CNRM)/Centre Europeen de Recherche et Formation Avancees en Calcul Scientifique	$0.5° \times 0.5°$	91	r1i1p1f2
3.	EC-Earth3P	EC-EARTH Consortium	$0.7° \times 0.7°$	91	r1i1p2f1
4.	EC-Earth3P-HR	EC-EARTH Consortium	$0.35° \times 0.35°$	91	r1i1p2f1
5.	HadGEM3-GC31-HH	UK Met Office Hadley Centre (MOHC)	$0.23° \times 0.35°$	85	r1i1p1f1
6.	HadGEM3-GC31-HM	UK Met Office Hadley Centre (MOHC)	$0.23° \times 0.35°$	85	r1i1p1f1
7.	HadGEM3-GC31-MM	UK Met Office Hadley Centre (MOHC)	$0.55° \times 0.83°$	85	r1i1p1f1
8.	HadGEM3-GC31-LL	UK Met Office Hadley Centre (MOHC)	$1.25° \times 1.875°$	85	r1i1p1f1

1981–2010. The future projections are available for shared socio-economic pathway (SSP) 5–8.5, which represents the high emission scenario (O'Neill *et al.* 2017). Bias correction for raw temperature and rainfall data from climate model is carried out using the quantile mapping method (Ines & Hansen 2006).

Results from Khadka *et al.* (2022) suggest that the maximum and minimum temperature in the study basin will increase by 1.45 °C (0.8–1.9 °C) and 1.54 °C (1.1–1.9 °C) in the near-future compared to the baseline. While there will be no significant changes (0.5%, between −5 and +10%) in the annual rainfall, temporal variations will increase in the future with projected increase by 6–11% and decrease in the summer by 2–8%. Similarly, the ensemble of the selected climate models indicated that the extreme rainfall events, computed as 10-year return values of 1-day maximum and 5-day consecutive maximum rainfall, will increase by 23% (9–40%) in the near-future period. The results are suggestive of significant impacts of climate change on the rainfall extremes.

2.5. Methodology

Figure 3 presents the overall methodology used in the study. SPEI is used to characterize droughts in terms of duration, severity and frequency. Multi-variate analysis is then carried out to quantify the drought hazard. Similarly, six physiographic and climatic factors have been utilized to produce the flood hazard maps. Joint flood and drought hazard map is prepared by combining the individual hazard maps in ArcMap 10.6.1 (ESRI). Climate change projections (including the extreme rainfall) are taken from the study by Khadka *et al.* (2022). The detailed methodology is explained in the following sub-sections.

2.6. Current and future flood hazard

The first phase of the methodology was a literature review of papers (2004–2021) covering articles using MCDA-GIS for flood hazard and risk (Figure 4 and Supplementary material, Table S1). This methodology was chosen as it is frequently used within the literature (Tanavud *et al.* 2004; Duan *et al.* 2009; Ozturk & Batuk 2011; Paquette & Lowry 2012; Elsheikh *et al.* 2015; Rahmati *et al.* 2016; Samanta *et al.* 2016; Alves *et al.* 2018; Ghosh & Kar 2018; Tang *et al.* 2018; Liu *et al.* 2019; Nigusse & Adhanom 2019; Shadmehri Toosi *et al.* 2019, 2020; Vavatsikos *et al.* 2019; Ajjur & Mogheir 2020; Kittipongvises *et al.* 2020; Kongmuang *et al.* 2020; Feizizadeh *et al.* 2021) and provides the ability to weight and combine multiple inputs to create an integrated analysis. Using the driving factors that appeared repeatedly within the literature,
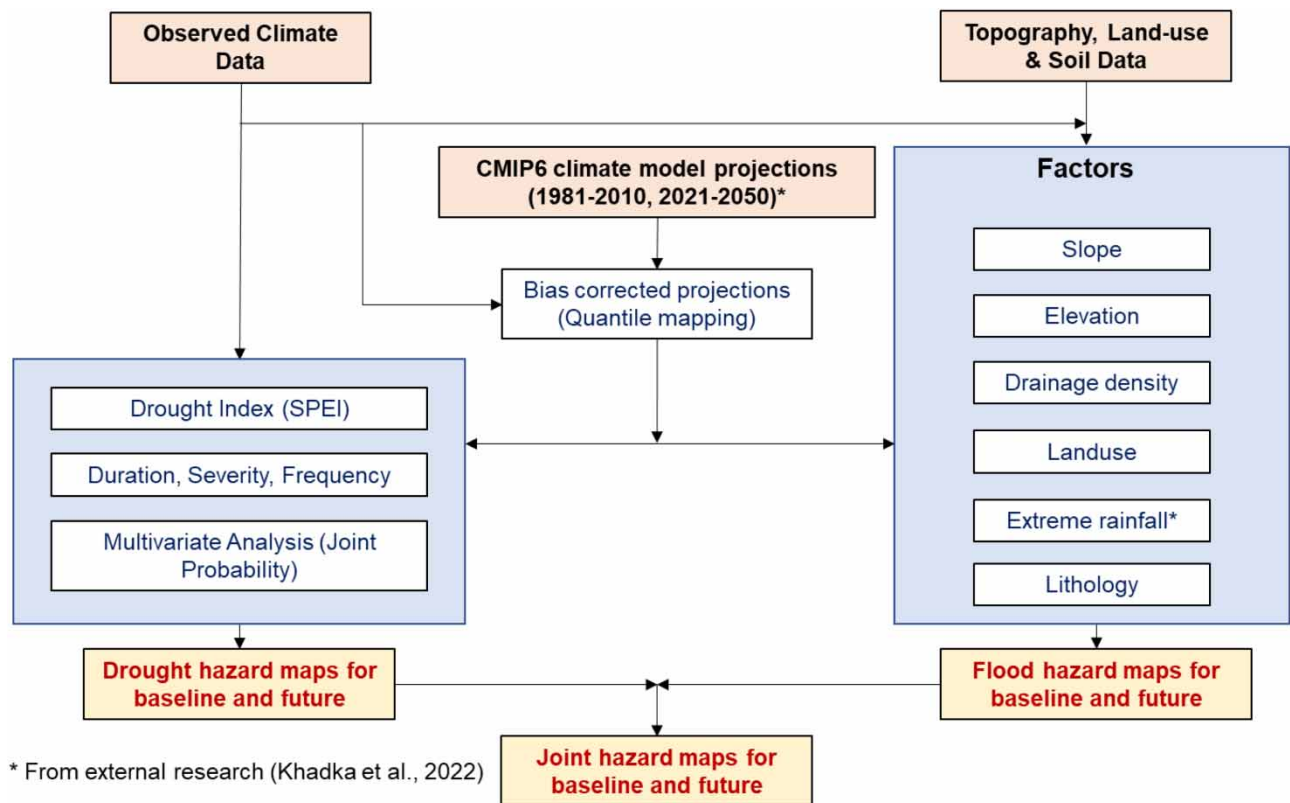

Figure 3 | Overall methodology for preparing the joint hazard maps for observed and climate change scenarios.
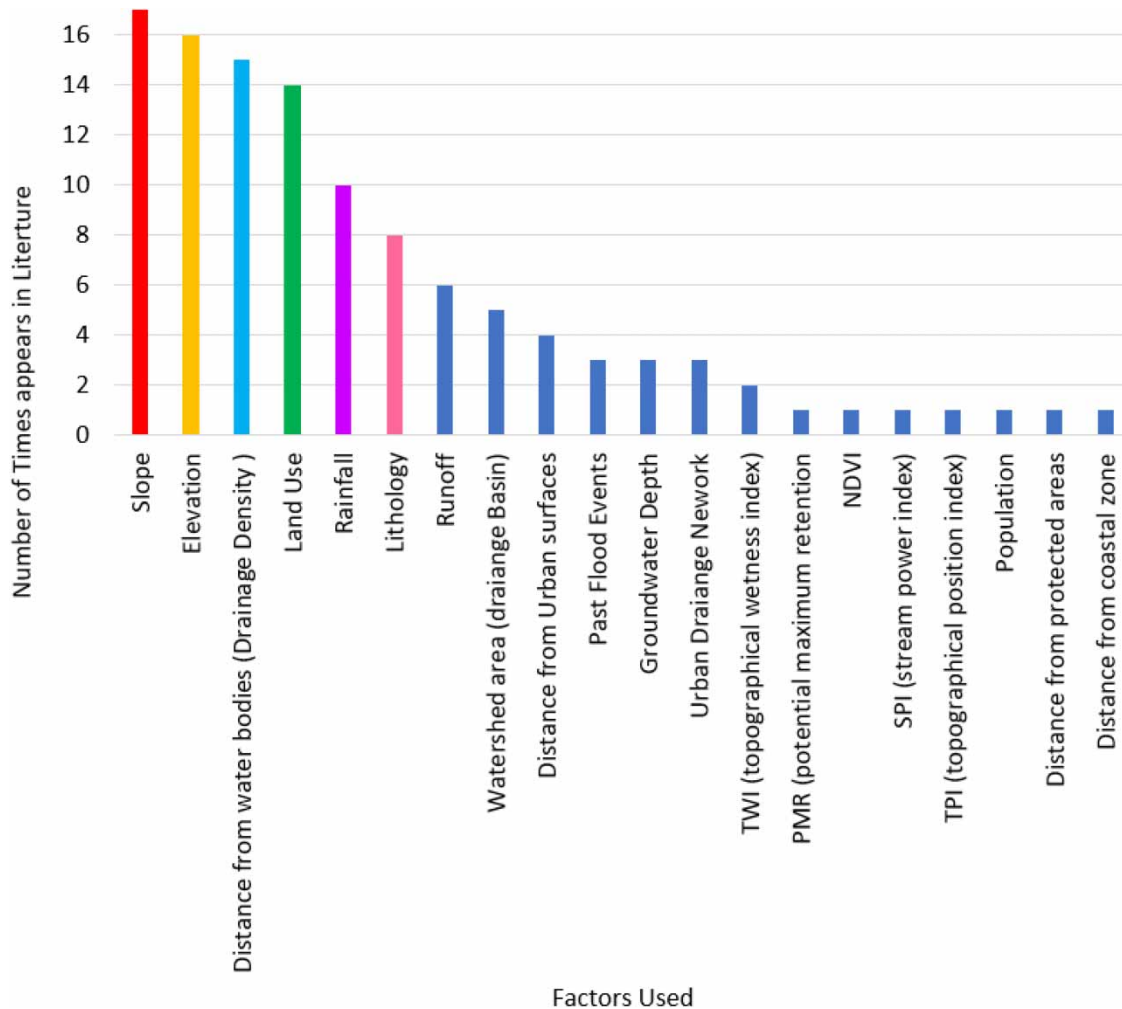
Figure 4 | Factors used within the MCDA-GIS literature for flood-related risk or hazard analysis. The first six driving factors used were slope, elevation, distance from water bodies (drainage density), land use, rainfall, and lithology.

the top six were selected: slope, elevation, distance from water bodies (drainage density), land use, rainfall and lithology (Figure 4). Other factors that appeared in the literature included distance from urban area, urban drainage network, population and distance from coastal zone; these factors were disregarded from the study as the catchment is primarily agricultural and land locked. Others such as groundwater depth, Topographical Wetness index (TWI), Potential maximum Retention (PMR) and SPI could not be used due to the limited data pool available to the study.

The weighting for driving factors can be decided via questioning from a series of experts or stakeholders (Alves *et al.* 2021); however, for this case study, the six chosen driving factors were considered equal weights (Januadi & Nabila 2020).

The ArcMap spatial analysis weighted sum tool was used to overlay several raster layers of factors presented in Figure 3. By multiplying each by a given weight and summing them together so the sum of all weights equalled 100%, a single flood hazard map was created. Each raster map within the analysis was reassigned a reclassified to identify the preference for the class relative to the criterion in the overlay analysis (Table 3). Topographic maps were reclassified from 1 to 5 according to the Jenks natural break method (Vojinovic *et al.* 2016; Shadmehri Toosi *et al.* 2019, 2020; Kong-muang *et al.* 2020). Rainfall extremes are the main driver of flooding events. In this study, 10-year return values of annual maximum consecutive 5-day rainfall (RX5day) are used as a climatic factor for assessing future flood hazards. It is one of the extreme rainfall indices recommended by 'The Expert Team on Climate Change Detection and Indices' (ETCCDI) (Peterson 2005). As shown in Figure 5, the extreme rainfall represented by RX5day is projected to increase under climate change scenarios. CNRM-CM6-1 projects a least increase in RX5day (6%), while the highest increases are projected by

Table 3 | Classification of flood hazard levels based on normalized values for topographic factors – reclassified via the Jenks natural break method

| Thematic layer	Classified value	Reclassified value	Level of hazard
Elevation	64–140	5	Very high hazard
	140–160	4	High hazard
	160–186	3	Medium
	186–241	2	Low hazard
	241–1,356	1	Very low hazard
Slope	0–0.0755	1	Very low hazard
	0.0755–0.2266	2	Low hazard
	0.2266–0.4533	3	Medium
	0.4533–1.0577	4	High hazard
	1.0577–19.264	5	Very high hazard
Drainage density (distance from river)	0–2,105	5	Very high hazard
	2,105–4,975	4	High hazard
	4,975–8,803	3	Medium
	8,803–14,352	2	Low hazard
	14,352–48,800	1	Very low hazard
Land use	Forest/Miscellaneous	1	Very low hazard
	Perennial and orchard	2	Low hazard
	Field crops	3	Medium
	Paddy field	4	High hazard
	Water bodies, Marshland, urban	5	Very high hazard
Soil types	Sand	1	Very low hazard
	Sandy loam	2	Low hazard
	Sandy loam/clay loam	3	Medium
	Loam	3	Medium
	Clay loam/loam	4	High hazard
	Clay loam	4	High hazard
	Clay	5	Very high hazard
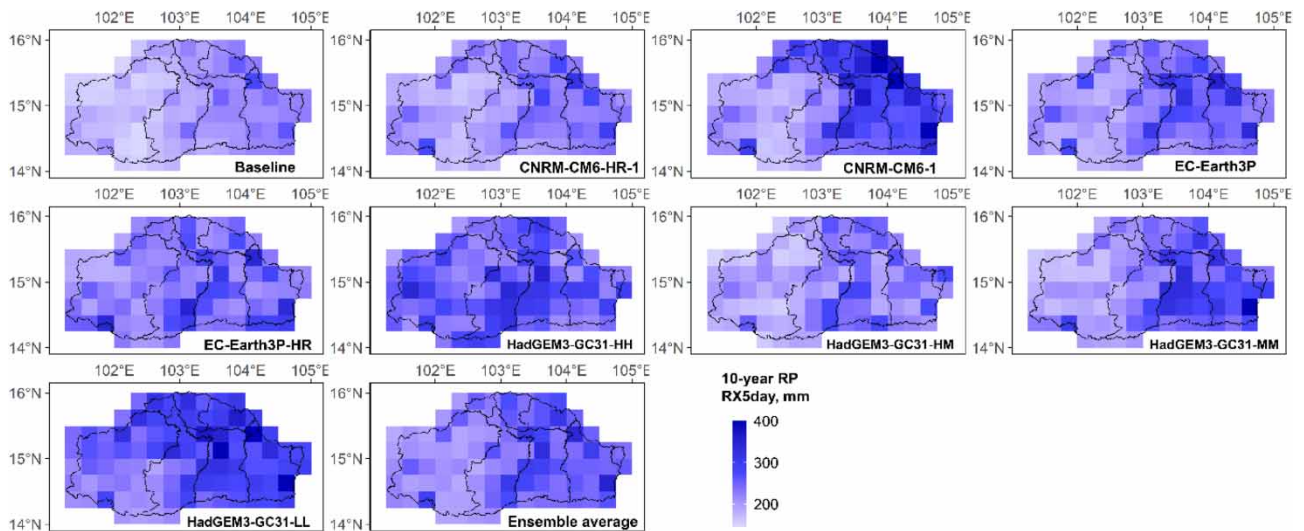
Figure 5 | The 10-year return values (RP) of annual maximum consecutive 5-day rainfall (RX5day) for the baseline period and for the near-future period using eight climate models and the ensemble average.

HadGEM3-GC31-HH (51%) and HadGEM3-GC31-LL (34%) in the near-future. Rainfall maps were created using Empirical Bayesian kriging (EBK). A study by Ali *et al.* (2021) assessed the optimal spatial distribution and rainfall characterization of 27 interpolation techniques from geo-statistical and deterministic categories and concluded that EBK was a robust and straightforward interpolation technique that requires minimal interactive modelling. Subsequently, EBK was used as the interpolation technique for the rainfall maps.

2.7. Current and future drought hazard

To characterize the drought events in the basin, SPEI (Vicente-Serrano *et al.* 2010) has been used. It is a multi-scalar meteorological drought index, which considers climatic water balance [i.e., difference between precipitation (P) and potential evapotranspiration (PET)]. Since it considers both temperature and precipitation, it is suitable for climate change analysis. PET is estimated using the Hargreaves–Samani (Hargreaves & Samani 1982) method. Although the SPEI can be calculated at different timescales, a 12-month timescale is more relevant for climate change studies (Ahmadalipour *et al.* 2017; Lee *et al.* 2019) so that short-term rainfall variabilities can be avoided. SPEI is calculated by fitting the data in GEV distribution (Stagge *et al.* 2015; Khadka *et al.* 2021).

Droughts are characterized in terms of duration, severity and frequency. In order to avoid the minor drought events, a SPEI threshold method suggested by Khadka *et al.* (2021) has been used. This method uses two criteria to define droughts: (a) a certain length of consecutive period has SPEI less than zero, and (b) the maximum intensity during that period is ≤ -0.5. The method will omit minor events while preserving the duration and severity characteristics. Univariate analysis of drought duration and severity is widely practiced (Liu *et al.* 2011; Chen *et al.* 2013; Sun *et al.* 2019), but since duration and severity are highly correlated (Masud *et al.* 2015; Khadka *et al.* 2021), it is often prudent to consider them together. In this study, a multi-variate approach using the copula function (Sklar 1959) is used to determine the drought hazard. The joint return period of drought events with severity (S) exceeding 's' and duration (D) exceeding 'd' is given by the following equation (Shiau 2006):

$$T_{s,d} = \frac{E(L)}{1 - F(s) - F(d) + C(s, d)}. \tag{1}$$

The denominator represents the joint occurrence probability P ($D > d$ and $S > s$), with chosen thresholds of duration (d) and severity (s) taken as the median values of univariate frequency analysis; $F(s)$ and $F(d)$ are the cumulative probability of the drought event exceeding severity of 's' and duration of 'd'; $E(L)$ is the average or expected drought interval. Following Nelson 2006, the empirical copula function [$C(s,d)$] of two random variables, x and y, is derived as:

$$C\left(\frac{i}{n}, \frac{j}{n}\right) = \frac{\# (x \leq x_{(i)},\ y \leq y_{(j)})}{n} = \frac{m}{n}, \tag{2}$$

where x_i and y_j are the order statistics of the samples of size n and m is the number of observations satisfying $x \leq x_i$ and $y \leq y_j$, with $1 \leq i, j \leq n$. The joint probability of the 10-year joint return drought event is considered to define the drought hazard.

2.8. Normalization and categorization

Computed factors for the flood hazard and the joint probability for the drought hazard are normalized between 0 and 1 before the hazards are classified into five equal-spaced categories (Table 4),

$$X_{(i)\ normalized} = \frac{(X_i - X_{min})}{(X_{max} - X_{min})}, \tag{3}$$

where X_i is the factor/joint probability for grid i, and X_{min} and X_{max} are the minimum and maximum values among all grids, respectively. Normalization for the climate change scenario is carried out with respect to the baseline period.

Table 4 | Classification of flood/drought hazard levels based on normalized values

Normalized value	Class	Level of hazard
<0.2	1	Very low hazard
0.2–0.4	2	Low hazard
0.41–0.6	3	Medium hazard
0.61–0.8	4	High hazard
>0.8	5	Very high hazard

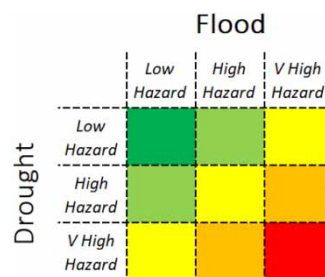## 2.9. Combined flood and drought hazards

The hazard score was calculated by combining the previous normalized flood and drought hazard maps using the ArcMap 10.6.1 mosaic to the new raster tool. As illustrated in Figure 6, each square represents a different level of hazard whether this be a single hazard (flood or drought) or a combined hazard (flood and drought), where the drought hazard was on the *y*-axis and the flood hazard was on the *x*-axis. The hazard level was determined based on these categories and given a colour code. Combined hazard maps were prepared for the baseline period, and for the future period, using the eight CMIP6 models (Table 2). A multi-model ensemble defined as the average was also created.

3. RESULTS AND DISCUSSION

3.1. Current and future flood hazard

There is a limited spatial variation in the locations of the flood hazard within the basin between the baseline period and future hazard (Figure 7) with CNRM-CM6-1, EC-Earth3P and HadGEM3-GC31-MM having the greatest resemblance to the multi-model ensemble. Overall, there is a low/very low flood hazard seen in the west (Nakhon Ratchasima) of the catchment and in the very south locations associated with increased elevations and degree of the slope level. Main areas of 'very high' to high flood hazards are seen in the east (Si Sa Ket) and north-eastern areas (Roi Et and Maha Sarakham), locations where elevations are the lowest, the slope is the steepest, and the distance from the river tributaries is smaller. It is well documented that an increase in the elevation reduces flooding propensity (Khalequzzaman 1994), whereas the slope influences the direction of and amount of surface runoff or subsurface drainage, having a dominant effect on the contribution of rainfall to stream flow. Consequently, steeper slopes are more susceptible to surface runoff, while flat terrains are susceptible to water logging (Ouma & Tateishi 2014).

For the near-future period, the majority of climate models suggest the increased 'very high' flood hazard area compared to the observed period with 11% classified as 'high' flood hazard (Figures 7 and 8). In particular, climate models HadGEM3-GC31-LL (19%) and HadGEM3-GC31-HH (17%) predicted the greatest increase in the 'very high' flood hazard area, whereas HadGEM3-GC31-HM (9%) predicted the least and less than the observed period. Areas of 'high' and 'medium' hazards have also increased, but this is less extreme varying from 22 to 24% and 26 to 28%, respectively, for the near-future period compared to the 22 and 27% for the observed period (Figure 8). Flood hazard increases are observed in the east of the basin especially in Rio Et and Si Sa Ket, correlating to areas where increasing rainfall was observed and along Mun tributaries within Nakhon Ratchasima and Buri Ram. This concurs with findings from Khadka *et al.* (2021) that the magnitude of extreme rainfall will increase in the future within all models except HadGEM3-GC31-HM. In addition, areas of very low

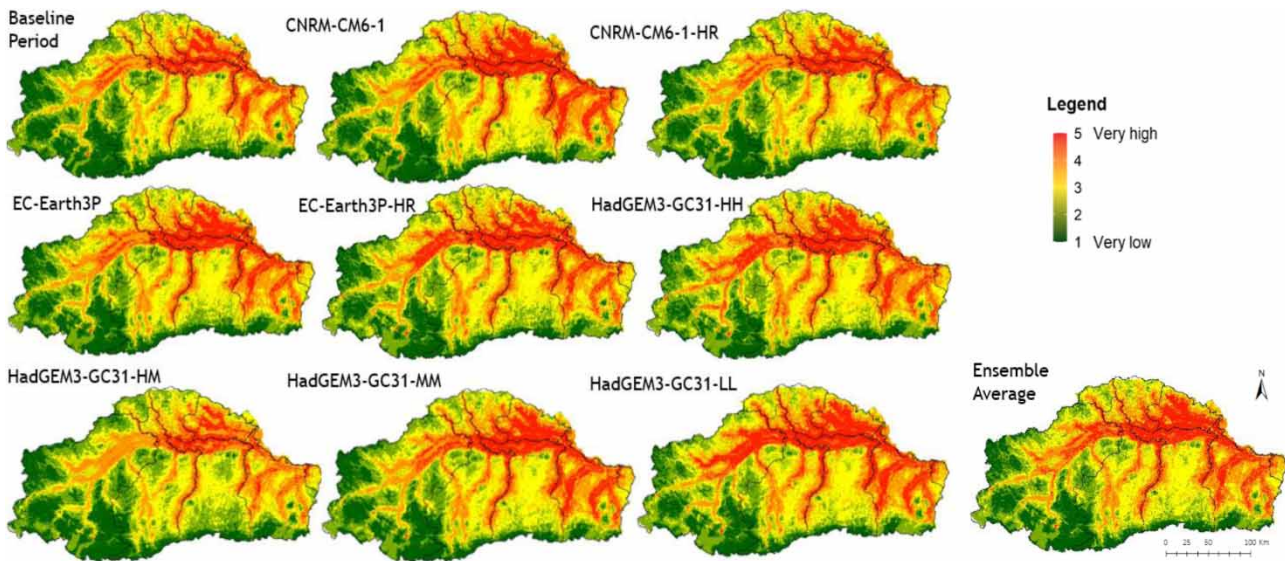**Figure 6** | Combined hazard matrix for flood and drought.

Figure 7 | Flood hazard map of the Mun River basin for the baseline period (1981–2010) and near-future period (2021–2050) using eight climate models and their ensemble. Hazards are classified into five classes: very low (1), low (2), medium (3), high (4), and very high (5).
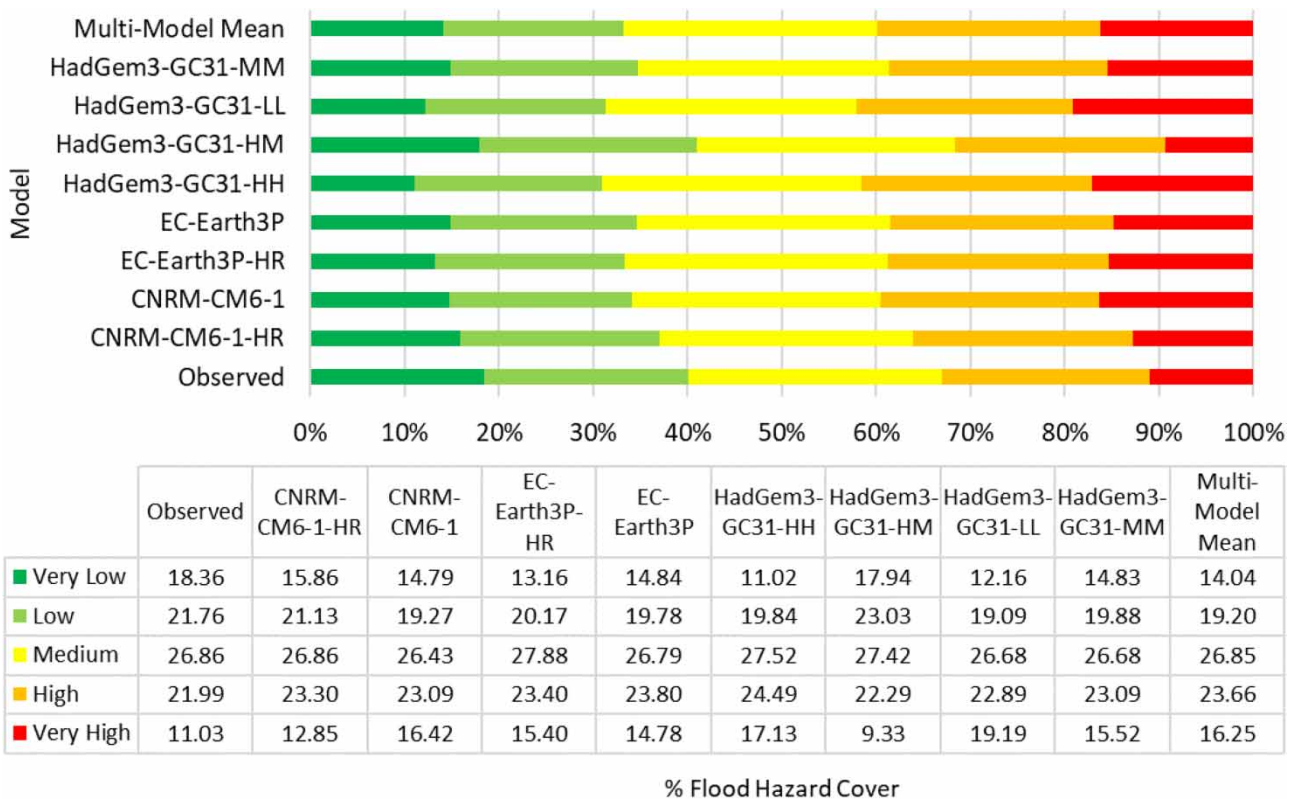

	Observed	CNRM-CM6-1-HR	CNRM-CM6-1	EC-Earth3P-HR	EC-Earth3P	HadGem3-GC31-HH	HadGem3-GC31-HM	HadGem3-GC31-LL	HadGem3-GC31-MM	Multi-Model Mean
■ Very Low	18.36	15.86	14.79	13.16	14.84	11.02	17.94	12.16	14.83	14.04
■ Low	21.76	21.13	19.27	20.17	19.78	19.84	23.03	19.09	19.88	19.20
■ Medium	26.86	26.86	26.43	27.88	26.79	27.52	27.42	26.68	26.68	26.85
■ High	21.99	23.30	23.09	23.40	23.80	24.49	22.29	22.89	23.09	23.66
■ Very High	11.03	12.85	16.42	15.40	14.78	17.13	9.33	19.19	15.52	16.25

% Flood Hazard Cover

Figure 8 | Percentage area (%) under different hazard levels for the observed period (1981–2010) and near-future period (2021–2050) using eight climate models and their ensemble.

to low flood hazard have decreased in all future scenarios compared to the observed period (18%), especially within HadGEM3-GC31-LL (11%) and HadGEM3-GC31-HH (12%). Locations for this decrease in the flood hazard are observed in the south catchments Buri Ram and Surin (Figures 7 and 8).

While the higher resolution version of CNRM-CM6-1-HR shows a reduced flood hazard (Figure 8) compared to the multi-model ensemble, both models agreed that the flood hazard will increase in the basin. This corresponds to where the projected increase in the rainfall is 10%. The results from the two models from EC-Earth Consortium are dissimilar, with Earth3P-HR finding an increase in the 'very high' flood hazard area in Nakhon Ratchasima compared to EC-Earth3P. Nevertheless, percentage-wise (Figure 8) the two models have similar results, although the high-resolution version of the model does find a slight increase in the % area covered by 'very high', 'medium' and 'low' flood hazards (Figure 8).

3.2. Current and future drought hazard

Drought hazard maps of the study area are created for the baseline period (1981–2010) as well as for the near-future period (2021–2050) using the multi-variate approach are shown in (Figure 9). While the results on drought hazard only are presented here, the detailed analyses of the observed droughts are discussed in a study by Khadka et al. (2021).

There is a significant variation in the drought hazard level within the basin during the baseline period [Figure 9(a)]. Nakhon Ratchasima (western part) has the higher area under the 'very high' hazard category, while Nakhon Ratchasima, Si Sa Ket (eastern part) and Roi Et (north-eastern part) have a significant area under the 'high' drought hazard category. Buriram, Surin and Maha Sarakham provinces have a relatively 'low' drought hazard in the basin. Overall, it can be observed that the drought hazard in the basin is irrespective of the annual rainfall received by the area. For example, Si Sa Ket receives the highest annual rainfall, but a significant area is under 'high' and 'very high' drought hazard levels. Drought characteristics and, hence, drought hazards are more affected by the temporal variability of the climatic parameters.

For the near-future period, most of the climate models (except CNRM-CM6-1-HR and HadGEM3-GC31-LL) have consensus that the 'high' and 'very high' hazards area will significantly increase and mostly concentrate on the western part of the basin. The multi-model ensemble also indicates the dire scenario where hazard levels have increased significantly throughout the basin. Table 5 shows that the area under high and 'very high' drought hazard levels will increase from 27 and 4% during the baseline period to 43 and 37% during the near-future period (multi-model ensemble average), respectively. All of the climate models (except CNRM-CM6-1-HR) suggest that the area with 'low' and 'very low' drought hazards will decrease in the near-future. High-resolution version of climate models from Met Office Hadley Centre (MOHC) and EC-Earth Consortium projected a significant increase in the area with a 'very high' drought hazard level, while the model from CNRM projected least increase. Spatially, the high-resolution version of the model from CNRM shows a reduced hazard in the eastern part of the basin (where the projected increase in the annual rainfall is 10%); both versions agree that the drought hazard will increase in the western part. The results from two models from EC-Earth Consortium are similar, even though the low-
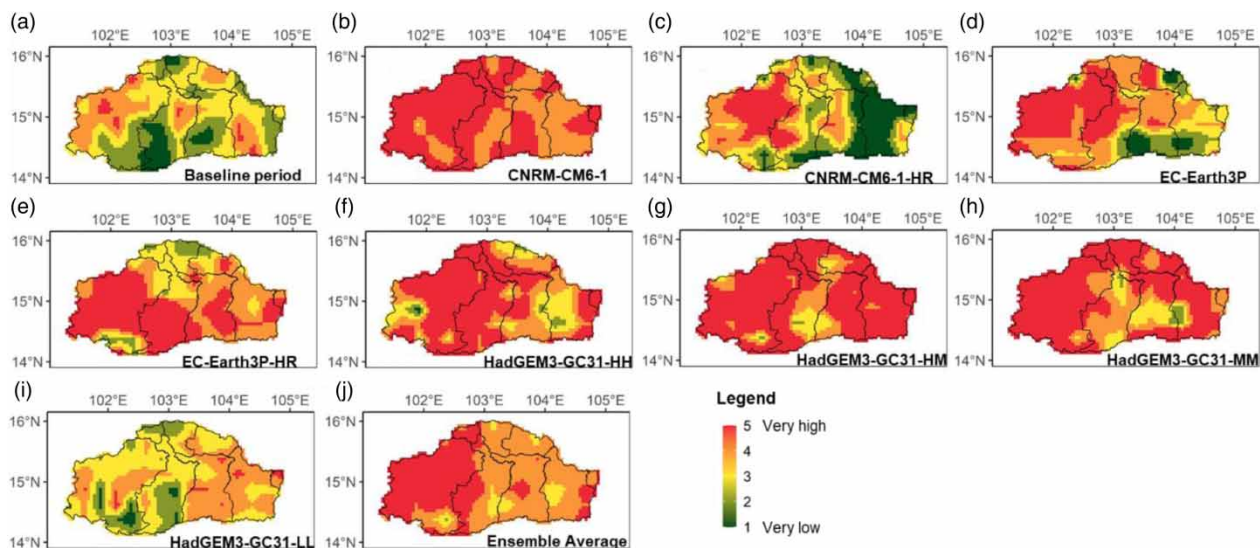

Figure 9 | Drought hazard map of the Mun River basin for the baseline period (1981–2010) and near-future period (2021–2050) using eight climate models and their ensemble. Hazards are classified into five classes: very low (1), low (2), medium (3), high (4), and very high (5).

Table 5 | Projected area of the Mun River basin (in %) under different drought hazard levels during observed and near-future period

Hazard level			Very low	Low	Medium	High	Very high
Area under different hazard levels (%)	Observed period		8	26	36	27	4
	Near-future period (2021–2050)	CNRM-CM6-1-HR	23	15	17	11	34
		CNRM-CM6-1	0	17	17	8	57
		EC-Earth3P-HR	0	1	11	18	70
		EC-Earth3P	6	9	12	18	55
		HadGEM3-GC31-HH	0	2	9	20	68
		HadGEM3-GC31-HM	0	0	4	17	79
		HadGEM3-GC31-LL	0	2	35	41	22
		HadGEM3-GC31-MM	3	14	32	30	21
		Ensemble average	0	2	18	43	37

resolution version shows a low hazard in the south-east part. Except the low-resolution version of the model from the MOHC, three models project a considerable increase in the drought hazard in the basin.

Under a climate change scenario, future droughts are projected to be longer (increase of 22%) and severe (increase of 63%), while the joint occurrence probability of the drought event, which exceeds the 10-year return period threshold of duration and severity, is also projected to increase by 37% (Khadka *et al.* 2022). These are mainly driven by an increase in evapotranspiration (by approximately 5%) and higher temporal variability of the rainfall (increase by approximately 35%). Consequently, areas under 'high' and very high drought hazards are projected to increase in the basin. The results concur with the findings by Khadka *et al.* (2022), which shows that the increase in the magnitude of the extreme events will be much higher than the increase in the average climate.

3.3. Current and future combined hazards

Floods and droughts are the two major natural hazards that create significant impacts on people lives and their well-being; it is already well established that the Mun River basin suffers from both at different periods (Prabnakorn 2020). Single hazard areas from the observed period to the near-future decrease dramatically and increase depending on the climate model (Figure 10), decreasing from 40% for the observed to 4% for the multi-model ensemble. Furthermore, areas classified as a low combined hazard have also decreased from 30% of the catchment to 20% of the catchment for the observed and ensemble mean, respectively. However, more harrowing findings are that areas of the combined hazard of medium and above have increased significantly, especially for 'medium' and 'high' rising from 20 and 9% to 51 and 20% for the observed period and multi-model ensemble, respectively. Overall, this means that over 75% (76%) of that catchment will be covered by combined hazards from 'medium' to 'very high' hazard levels compared to the 30% in the observed period. This is a percentage increase in the area of 155%.

Results found that in the near-future period, 'very high' combined hazards will be located in Nakhon Ratchasima and in the north provinces of Rio Et, Khon Kean and Maha Sarakham. The greatest 'very high' and 'high' combined hazard is seen in HadGEM3-GC31-HH (13% + 20%) and the two models from EC-Earth Consortium: Earth3P-HR (10 and 21%) and Earth3P (8 and 18%) (Figures 10 and 11). Generally, the combined hazards will be worst in the west (Nakhon Ratchasima), and this is the area where drought hazards increase (Figure 9); however, HadGem3-GC31-HM and HadGem3-GC31-MM exclude this reasoning finding hazard reduced in the west compared to the observed period. The models HadGem3-GC31-HM and CNRM-CM6-1-HR display the least increase in the combined hazard area and actually found a decrease in the 'very high' combined hazard (1.2 and 1.3% areas, respectively) compared to that observed at 1.4% (Figure 11). Areas of 'very high' combined hazards are in locations that follow the river route or are in close proximity to the river, where flood hazards were observed (Figures 1 and 10). Compared to the baseline period, the near-future multi-model ensemble finds an increase in the overall hazard across the catchment of at least one level (Figure 11); this is most prominent in the west – Nakhon Ratchasima and Buri Ram, and north-eastern provinces – Khon Kean, Roi Et and Maha Sarakham (Figure 10). On the other hand, Si Sa Ket finds a similar combined hazard to the baseline period.

Although we present how agriculture faces multiple challenges in terms of floods and droughts, we also want to point challenges for the critical infrastructure (CI) (Kumar *et al.* 2021a). The IPCC states that climate change unequivocally impacts
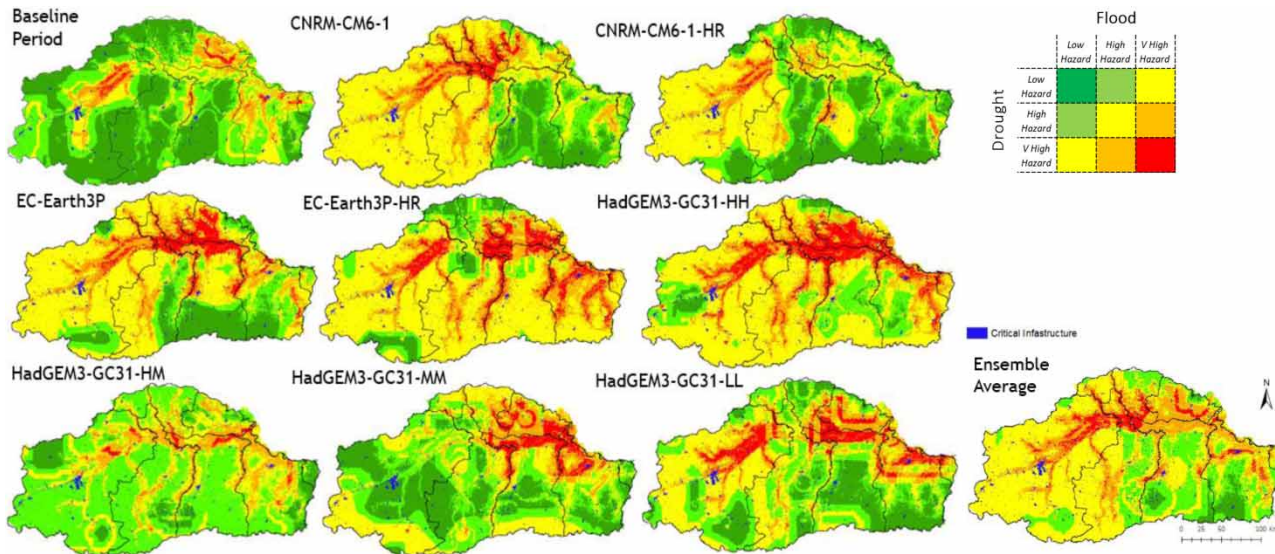
Figure 10 | Combined flood and drought hazard maps of the Mun River basin for the baseline period (1981–2010) and near-future period (2021–2050) using eight climate models and their ensemble. Hazard maps also display locations of the critical infrastructure identified as cities, communications, utilities, and industrial and institutional lands by the Land Development Department of Thailand for the years 2016–2017.
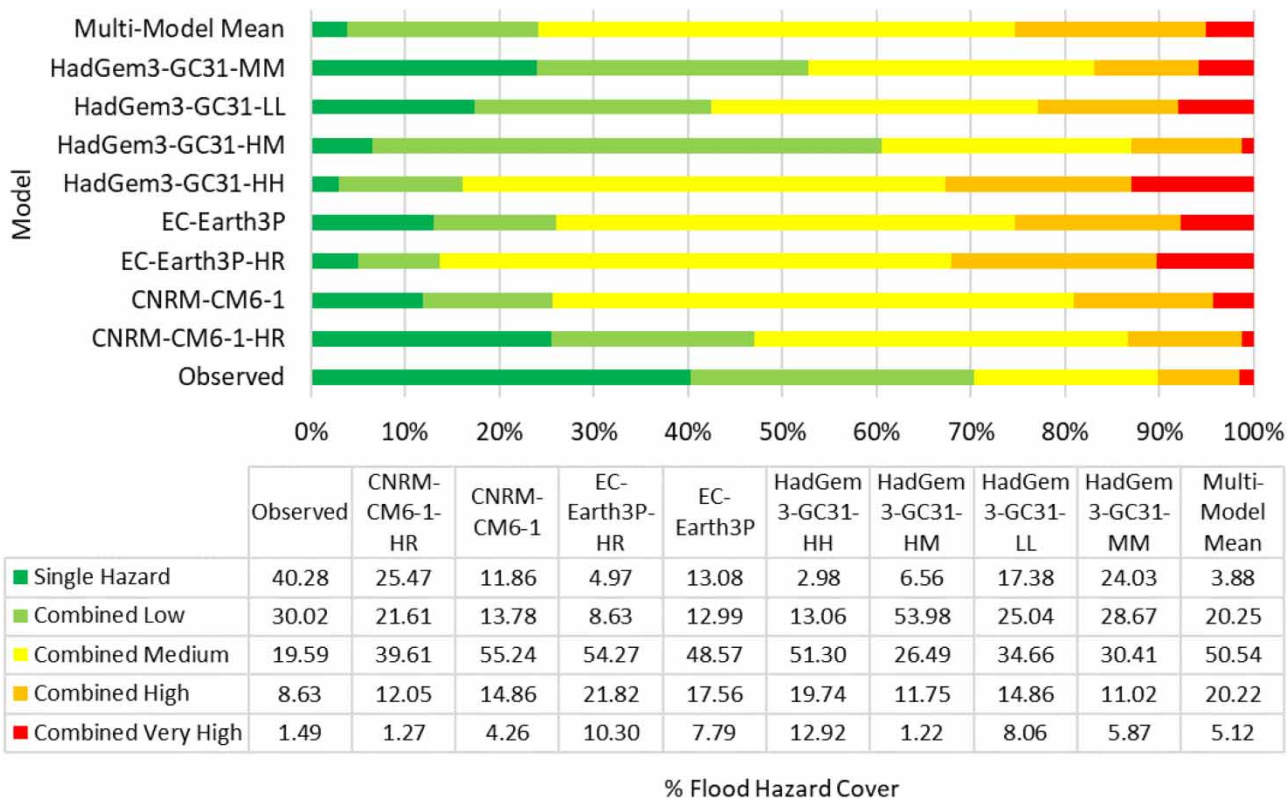

	Observed	CNRM-CM6-1-HR	CNRM-CM6-1	EC-Earth3P-HR	EC-Earth3P	HadGem3-GC31-HH	HadGem3-GC31-HM	HadGem3-GC31-LL	HadGem3-GC31-MM	Multi-Model Mean
Single Hazard	40.28	25.47	11.86	4.97	13.08	2.98	6.56	17.38	24.03	3.88
Combined Low	30.02	21.61	13.78	8.63	12.99	13.06	53.98	25.04	28.67	20.25
Combined Medium	19.59	39.61	55.24	54.27	48.57	51.30	26.49	34.66	30.41	50.54
Combined High	8.63	12.05	14.86	21.82	17.56	19.74	11.75	14.86	11.02	20.22
Combined Very High	1.49	1.27	4.26	10.30	7.79	12.92	1.22	8.06	5.87	5.12

% Flood Hazard Cover

Figure 11 | Percentage combined hazard cover for flood and drought hazard maps of the Mun River basin for the observed period (1981–2010) and near-future period (2021–2050) using eight climate models and the multi-ensemble mean.

various aspects of the built environment: transport, energy, water/wastewater and communications (Hawchar *et al.* 2020). Therefore, we argue that it is also essential to gain an understanding of CI vulnerability to climate-related threats (current and future), in order to develop effective strategies to enhance the resilience of CI (Hawchar *et al.* 2020; Schipper 2020). Floods and droughts can cause both direct (direct damage to physical infrastructure) and indirect effects (hindering supply chains and raw material production) (Kumar *et al.* 2021a). The current CI within the Mun River basin for the baseline period is situated in 'high' multi-hazardous areas, for example, Nakhon Ratchasima, Surin and Si Sa Ket (Figure 10). It is likely in the future with land use changes, CI development (cities, communications, utilities, and industrial and institutional lands) will increase across the catchment (Penny *et al.* 2021). Steps towards mitigating hydro-meteorological hazards could include nature-based solutions (NBS) (Majidi *et al.* 2019; Kumar *et al.* 2021b; Vojinovic *et al.* 2021). A study by Penny *et al.* (2023) provides an extension of this research, which looks into NBS for the Mun River basin. Nevertheless, caution must be taken as though adaptation to climate change is necessary, if adaptation strategies fail, this can worsen situations, leading to maladaptation (Schipper 2020).

4. RECOMMENDATIONS AND FUTURE STUDY

We recommend that a future study may also consider (i) using additional indices, (ii) different weights' allocation for the hazard indexes, and (iii) other methods such as NDVI and LSWI, or (iv) investigating the role of antecedent rainfall and soil moisture conditions (Ávila 2015; Navarathinam *et al.* 2015) in flood hazards. Currently, the present work only considers physiographic variables at a certain point, focusing more on local flooding. However, we also see that the work could be improved by including variables that affect the flood hazard originating from upstream, localized flooding, i.e., flood waters that occur upstream of the catchment but, in fact, affect the flood hazard within the catchment area, for example, stream flow. For this, we recommend to consider studies that have included flow accumulation within their MCDA-GIS methodologies for assessing flood hazard and/or risk, including Nandi *et al.* 2016; Ozkan & Tarhan 2016; Kabenge *et al.* 2017; Dash & Sar 2020; Dung *et al.* 2022; and Baykal *et al.* 2023. In addition to the above, the work could be taken further by using a hydrologic-hydrodynamic model and or 'Bluespot' analysis (Balstrøm 2022; Penny *et al.* 2023).

We acknowledge that this study could be enhanced by using methodologies such as Saaty AHP and ANP (de Brito *et al.* 2018), and rather than using equal weights (used in this study), individual weighting or proportional scoring for MCDA-GIS variables should be used. Nevertheless, when compared to outcomes from other researchers, Khadka *et al.* (2021, 2022) and Prabnakorn (2020), both flood and drought are in agreement with similar studies/forecasts carried out in the Mun River basin. This consolidates/validates the methodology used here.

Formulation and implementation of necessary drought and flood adaptation plans in the basin has paramount importance in making the society more resilient. Provision of high efficiency irrigation systems by the integrative use of surface and groundwater resources could be a major step to combat the negative impacts of droughts in the near-future. Combining temporary storage solutions for excess flood waters in the open fields and increasing swamp/wetland areas could help store flood waters and recharge groundwater aquifers, in turn, combating drought.

5. CONCLUSION

The study has assessed individual and joint hazard levels of floods and droughts in the Mun River basin, Thailand, for baseline (1981–2010) and the near-future period (2021–2050). The flood hazard is computed using six physiographic and climatic factors. The method used for the flood hazard is useful for data-scarce regions, particularly when hydrologic and hydraulic modelling is not available and when rapid assessment is required. Similarly, the spatial drought hazard was assessed using the multi-variate approach that combines three drought characteristics (duration, severity and frequency). A joint hazard map is created by combining the information of drought and flood hazards.

Overall, there is a limited variation in the locations of flood hazard; however, between the baseline and near-future period, the majority of climate models suggest an increase in the 'high' and 'very high' flood areas. The area under 'high' and 'very high' flood hazard levels increases from 11 and 22% during the baseline period (1981–2010) to 16 and 24% during the near-future period (2021–2050), respectively. Flood hazard increases are observed in lower elevations in the east of the basin especially in Roi Et and Si Sa Ket, correlating to areas where increased extreme rainfall is predicted and along Mun River and its tributaries within Nakhon Ratchasima and Buri Ram.

Drought hazard during the baseline period shows an uneven spatial distribution within the basin. While majority of Nakhon Ratchasima and Si Sa Ket have the 'high' drought hazard, Buriram, Surin and Maha Sarakham have low levels, not following the average rainfall trends, which decrease from east towards west. This shows that the drought hazards are more defined by the temporal variability of the climatic parameter (particularly rainfall) than the spatial variability. Results clearly show that the drought hazard levels as well as their spatial extents will increase in the near-future period. The ensemble of climate models suggests that area under 'high' and 'very high' drought hazard levels will increase from 27 and 4% during the baseline period (1981–2010) to 43 and 37% during the near-future period (2021–2050), respectively.

When combining flood and drought hazards together, compared to the baseline period, the multi-model ensemble finds an increased area of 155% in the overall hazard across the catchment, this is most prominent in the west – Nakhon Ratchasima and Buri Ram, and north-eastern provinces – Khon Kean, Roi Et and Maha Sarakham. In addition, the CI in the basin, particularly situated in Nakhon Ratchasima, Surin and Si Sa Ket, is also at risk from hydro-meteorological hazards. Thus, adaptation for multi-hazard within multiland uses, potentially in the form of NBS, is needed across the catchment not just for the primarily agricultural regions but for areas where the CI is located. Findings present a grim outlook on future floods and droughts in the basin, and this is particularly important as the majority of the population and land area are tied to agriculture, which at present are mostly rainfed cultivation systems. Thus, the results show that the agriculture sector in the basin is highly vulnerable.

To summarize, our research delivers an integrated assessment of flood and drought hazards within the Mun River basin, providing an important step in mitigating risks in multi-hazard environments, the results of which can be employed to test scenarios of measures to reduce the impacts of drought and flooding, and the purpose of which can not only improve predictions but also help inform decision-making. We have reaffirmed that multi-criteria analysis in the GIS environment can be extremely useful in real-world water-related applications.

ACKNOWLEDGEMENTS

DATA AVAILABILITY STATEMENT

Data cannot be made publicly available; readers should contact the corresponding author for details.

CONFLICT OF INTEREST

The authors declare there is no conflict.

REFERENCES

Aalijahan, M., Salahi, B. & Hatami, D. 2021 Investigating the relationship between changes in atmospheric greenhouse gases and discharge fluctuations in the Basin of Aras River. *Int. J. Geogr. Geogr. Educ. (IGGE)* **44**, 461–474.

Aalijahan, M., Karataş, A., Lupo, A. R., Efe, B. & Khosravichenar, A. 2023 Analyzing and modeling the spatial-temporal changes and the impact of GLOTI index on precipitation in the Marmara Region of Türkiye. *Atmosphere (Basel)* **14**. https://doi.org/10.3390/atmos14030489.

Ahmadalipour, A., Moradkhani, H. & Demirel, M. C. 2017 A comparative assessment of projected meteorological and hydrological droughts: Elucidating the role of temperature. *J. Hydrol.* **553**, 785–797. https://doi.org/10.1016/j.jhydrol.2017.08.047.

Ajjur, S. B. & Mogheir, Y. K. 2020 Flood hazard mapping using a multi-criteria decision analysis and GIS (case study Gaza Governorate, Palestine). *Arab. J. Geosci.* **13**. https://doi.org/10.1007/s12517-019-5024-6.

Ali, G., Sajjad, M., Kanwal, S., Xiao, T., Khalid, S., Shoaib, F. & Gul, H. N. 2021 Spatial–temporal characterization of rainfall in Pakistan during the past half-century (1961–2020). *Sci. Rep.* **11**, 1–16. https://doi.org/10.1038/s41598-021-86412-x.

Alves, P. B. R., de Melo Filho, H., Tsuyuguchi, B. B., Rufino, I. A. A. & Feitosa, P. H. C. 2018 Mapping of flood susceptibility in Campina Grande County – PB: A spatial multicriteria approach. *Bol. Ciencias Geod.* **24**, 28–43. https://doi.org/10.1590/S1982-21702018000100003.

Alves, P. B. R., Djordjević, S. & Javadi, A. A. 2021 An integrated socio-environmental framework for mapping hazard-specific vulnerability and exposure in urban areas. *Urban Water J.* **18** (7), 530–543. doi:10.1080/1573062X.2021.1913505.

Ávila, A. D. 2015 Representative rainfall thresholds for flash floods in the Cali river watershed, Colombia. *Nat. Hazards Earth Syst. Sci. Discuss.* **3**, 4095–4119. https://doi.org/10.5194/nhessd-3-4095-2015.

Balstrøm, T. 2022 *Model Bluespots to map Flood Risk [WWW Document]*. esri. https://learn.arcgis.com/en/projects/model-bluespots-to-map-flood-risk/?fbclid=IwAR2Nfune0XsWiUwxNdKKEWn2UP3CWvwGJt-I1S9LeyFlZ7Mf3Hug1auYDmE (accessed 11 January 2023).

Baykal, T., Şener, E. & Terzi, Ö. 2023 Application of analytical hierarchy process for flood risk analysis: A case study in Küçük Aksu River Basin (Antalya, Turkey). *Iran. J. Sci. Technol. - Trans. Civ. Eng.* https://doi.org/10.1007/s40996-023-01055-4.

Brunner, M. I., Slater, L., Tallaksen, L. M. & Clark, M. 2021 Challenges in modeling and predicting floods and droughts: A review. *Wiley Interdiscip. Rev. Water* **8**, 1–32. https://doi.org/10.1002/wat2.1520.

Burke, C. & Stott, P. 2017 Impact of anthropogenic climate change on the east Asian summer monsoon. *J. Clim.* **30**, 5205–5220. https://doi.org/10.1175/JCLI-D-16-0892.1.

Chandrasekar, K., Sesha Sai, M. V. R., Roy, P. S. & Dwevedi, R. S. 2010 Land Surface Water Index (LSWI) response to rainfall and NDVI using the MODIS vegetation index product. *Int. J. Remote Sens.* **31**, 3987–4005. https://doi.org/10.1080/01431160802575653.

Chen, H. & Sun, J. 2017 Anthropogenic warming has caused hot droughts more frequently in China. *J. Hydrol.* **544**, 306–318. https://doi.org/10.1016/j.jhydrol.2016.11.044.

Chen, L., Singh, V. P., Guo, S., Mishra, A. K. & Guo, J. 2013 Drought analysis using copulas. *J. Hydrol. Eng.* **18**, 797–808. https://doi.org/10.1061/(ASCE)HE.1943-5584.0000697.

Chitwatkulsiri, D., Miyamoto, H. & Weesakul, S. 2021 Development of a simulation model for real-time urban floods warning: A case study at Sukhumvit Area, Bangkok, Thailand. *Water* **13**, 17.

Crausbay, S. D., Ramirez, A. R., Carter, S. L., Cross, M. S., Hall, K. R., Bathke, D. J., Betancourt, J. L., Colt, S., Cravens, A. E., Dalton, M. S., Dunham, J. B., Hay, L. E., Hayes, M. J., McEvoy, J., McNutt, C. A., Moritz, M. A., Nislow, K. H., Raheem, N. & Sanford, T. 2018 Defining ecological drought for the twenty-first century. *Bull. Am. Meteorol. Soc.* **98**, 2543–2550. https://doi.org/10.1175/BAMS-D-16-0292.1.

CRED. 2018 *Natural Disaster 2018*. Centre for Research on the Epidemiology of Disasters (CRED), Brussels.

Dash, P. & Sar, J. 2020 Identification and validation of potential flood hazard area using GIS-based multi-criteria analysis and satellite data-derived water index. *J. Flood Risk Manage.* **13**, 1–14. https://doi.org/10.1111/jfr3.12620.

Davenport, F. V., Burke, M. & Diffenbaugh, N. S. 2021 Contribution of historical precipitation change to US flood damages. *Proc. Natl. Acad. Sci. USA* **118**, 1–7. https://doi.org/10.1073/pnas.2017524118.

DDPM. 2015 *National Disaster Risk Management Plan*. Department of Disaster Prevention and Mitigation (DDPM).

de Brito, M. M., Evers, M. & Almoradie, A. D. S. 2018 Participatory flood vulnerability assessment: A multi-criteria approach. *Hydrol. Earth Syst. Sci.* **22**, 373–390. https://doi.org/10.5194/hess-22-373-2018.

Duan, M., Zhang, J., Liu, Z. & Aekakkararungroj, A. 2009 Use of remote sensing and GIS for flood hazard mapping in Chiang Mai Province, northern Thailand. In *Int. Conf. Geospatial Solut. Emerg. Manag. 50th Anniv. Chinese Acad. Surv. Mapp.* pp. 14–16.

Dung, N. B., Long, N. Q., Goyal, R., An, D. T. & Minh, D. T. 2022 The role of factors affecting flood hazard zoning using analytical hierarchy process: A review. *Earth Syst. Environ.* **6**, 697–713. https://doi.org/10.1007/s41748-021-00235-4.

Elsheikh, R. F. A., Ouerghi, S. & Elhag, A. R. 2015 Flood risk map based on GIS, and multi criteria techniques (Case study Terengganu Malaysia). *J. Geogr. Inf. Syst.* **07**, 348–357. https://doi.org/10.4236/jgis.2015.74027.

EM-DAT. 2019 *M-DAT: The OFDA/CRED International Disaster Database*. (accessed 2019) [WWW Document].

Fan, Y. & van den Dool, H. 2008 A global monthly land surface air temperature analysis for 1948–present. *J. Geophys. Res.* **113**, D01103. https://doi.org/10.1029/2007JD008470.

Feizizadeh, B., Gheshlaghi, H. A. & Bui, D. T. 2021 An integrated approach of GIS and hybrid intelligence techniques applied for flood risk modeling. *J. Environ. Plan. Manage.* **64**, 485–516. https://doi.org/10.1080/09640568.2020.1775561.

Forzieri, G., Feyen, L., Russo, S., Vousdoukas, M., Alfieri, L., Outten, S., Migliavacca, M., Bianchi, A., Rojas, R. & Cid, A. 2016 Multi-hazard assessment in Europe under climate change. *Clim. Change* **137**, 105–119. https://doi.org/10.1007/s10584-016-1661-x.

Gemmer, M., Jiang, T., Su, B. & Kundzewicz, Z. W. 2008 Seasonal precipitation changes in the wet season and their influence on flood/drought hazards in the Yangtze River Basin, China. *Quat. Int.* **186**, 12–21. https://doi.org/10.1016/j.quaint.2007.10.001.

Ghosh, A. & Kar, S. K. 2018 Application of analytical hierarchy process (AHP) for flood risk assessment: A case study in Malda district of West Bengal, India. *Nat. Hazards* **94**, 349–368. https://doi.org/10.1007/s11069-018-3392-y.

Guan, X., Zang, Y., Meng, Y., Liu, Y., Lv, H. & Yan, D. 2021 Study on spatiotemporal distribution characteristics of flood and drought disaster impacts on agriculture in China. *Int. J. Disaster Risk Reduct.* **64**, 102504. https://doi.org/10.1016/j.ijdrr.2021.102504.

Haarsma, R. J., Roberts, M. J., Vidale, P. L., Senior, C. A., Bellucci, A., Bao, Q., Chang, P., Corti, S., Fučkar, N. S., Guemas, V., von Hardenberg, J., Hazeleger, W., Kodama, C., Koenigk, T., Leung, L. R., Lu, J., Luo, J.-J., Mao, J., Mizielinski, M. S., Mizuta, R., Nobre, P., Satoh, M., Scoccimarro, E., Semmler, T., Small, J. & von Storch, J.-S. 2016 High resolution model intercomparison project (HighResMIP ∼ v1.0) for CMIP6. *Geosci. Model Dev.* **9**, 4185–4208. https://doi.org/10.5194/gmd-9-4185-2016.

Hammond, M., Chen, A., Djordjević, S. & Butler, D. 2014 Making cities more resilent to flooding. In: *Global Water Forum* "Collaborative Research on Flood Resilience in Urban Areas" (CORFU), Exeter, pp. 1–5.

Hargreaves, G. H. & Samani, Z. A. 1982 Estimating potential evapotranspiration. Technical note. *J. Irrig. Drain. Eng.* **108**, 225–230.

Hawchar, L., Naughton, O., Nolan, P., Stewart, M. G. & Ryan, P. C. 2020 A GIS-based framework for high-level climate change risk assessment of critical infrastructure. *Clim. Risk Manage.* **29**, 100235. https://doi.org/10.1016/j.crm.2020.100235.

Igarashi, K., Koichiro, K., Tanaka, N. & Aranyabhaga, N. 2019 Prediction of the impact of climate change and land use change on flood discharge in the song Khwae District, Nan Province, Thailand. *J. Clim. Change* **5**, 1–8. https://doi.org/10.3233/JCC190001.

Ines, A. V. M. & Hansen, J. W. 2006 Bias correction of daily GCM rainfall for crop simulation studies. *Agric. For. Meteorol.* **138**, 44–53. https://doi.org/10.1016/j.agrformet.2006.03.009.

Jacob, X. K., Bisht, D. S., Chatterjee, C. & Raghuwanshi, N. S. 2020 Hydrodynamic modeling for flood hazard assessment in a data scarce region: A case study of Bharathapuzha River Basin. *Environ. Model. Assess.* **25**, 97–114. https://doi.org/10.1007/s10666-019-09664-y.

Januadi, M. I. & Nabila, D. N. U. 2020 Routing the highway development by using SuperMap Least Cost Path Analysis (LCPA) and multi-criteria decision analysis (MCDA) and its assessment toward spatial planning. *IOP Conf. Ser. Earth Environ. Sci.* **561**. https://doi.org/10.1088/1755-1315/561/1/012019.

Kabenge, M., Elaru, J., Wang, H. & Li, F. 2017 Characterizing flood hazard risk in data-scarce areas, using a remote sensing and GIS-based flood hazard index. *Nat. Hazards* **89**, 1369–1387. https://doi.org/10.1007/s11069-017-3024-y.

Khadka, D., Babel, M. S., Shrestha, S., Virdis, S. G. P. & Collins, M. 2021 Multivariate and multi-temporal analysis of meteorological drought in the northeast of Thailand. *Weather Clim. Extrem.* **34**, 100399. https://doi.org/10.1016/j.wace.2021.100399.

Khadka, D., Babel, M. S., Collins, M., Shrestha, S., Virdis, S. G. P. & Chen, A. S. 2022 Projected changes in the near-future mean climate and extreme climate events in northeast Thailand. *Int. J. Climatol.* **42**, 2470–2492. https://doi.org/10.1002/joc.7377.

Khalequzzaman, M. D. 1994 Recent floods in Bangladesh: Possible causes and solutions. *Nat. Hazards* **9**, 65–80. https://doi.org/10.1007/978-94-011-0976-5_4.

Khan, D. M., Veerbeek, W., Chen, A. S., Hammond, M. J., Islam, F., Pervin, I., Djordjević, S. & Butler, D. 2018 Back to the future: Assessing the damage of 2004 Dhaka flood in the 2050 urban environment. *J. Flood Risk Manage.* **11**, S43–S54. https://doi.org/10.1111/jfr3.12220.

Kittipongvises, S., Phetrak, A., Rattanapun, P., Brundiers, K., Buizer, J. L. & Melnick, R. 2020 AHP-GIS analysis for flood hazard assessment of the communities nearby the world heritage site on Ayutthaya Island, Thailand. *Int. J. Disaster Risk Reduct.* **48**, 101612. https://doi.org/10.1016/j.ijdrr.2020.101612.

Komori, D., Rangsiwanichpong, P., Inoue, N., Ono, K., Watanabe, S. & Kazama, S. 2018 Distributed probability of slope failure in Thailand under climate change. *Clim. Risk Manage.* **20**, 126–137. https://doi.org/10.1016/j.crm.2018.03.002.

Kongmuang, C., Tantanee, S. & Seejata, K. 2020 Urban flood hazard map using GIS of Muang Sukhothai District, Thailand Article. *Geogr. Tech.* **15**, 143–152. https://doi.org/10.21163/GT.

Kumar, N., Poonia, V., Gupta, B. B. & Goyal, M. K. 2021a A novel framework for risk assessment and resilience of critical infrastructure towards climate change. *Technol. Forecast. Soc. Change* **165**, 120532. https://doi.org/10.1016/j.techfore.2020.120532.

Kumar, P., Debele, S. E., Sahani, J., Rawat, N., Marti-Cardona, B., Alfieri, S. M., Basu, B., Basu, A. S., Bowyer, P., Charizopoulos, N., Jaakko, J., Loupis, M., Menenti, M., Mickovski, S. B., Pfeiffer, J., Pilla, F., Pröll, J., Pulvirenti, B., Rutzinger, M., Sannigrahi, S., Spyrou, C., Tuomenvirta, H., Vojinovic, Z. & Zieher, T. 2021b An overview of monitoring methods for assessing the performance of nature-based solutions against natural hazards. *Earth-Science Rev.* **217**. https://doi.org/10.1016/j.earscirev.2021.103603.

Kwon, M. & Sung, J. H. 2019 Changes in future drought with HadGEM2-AO projections. *Water.* https://doi.org/10.3390/w11020312.

Lee, M. H., Im, E. S. & Bae, D. H. 2019 A comparative assessment of climate change impacts on drought over Korea based on multiple climate projections and multiple drought indices. *Clim. Dyn.* **53**, 389–404. https://doi.org/10.1007/s00382-018-4588-2.

Lesk, C., Rowhani, P. & Ramankutty, N. 2016 Influence of extreme weather disasters on global crop production. *Nature* **529**, 84–87. https://doi.org/10.1038/nature16467.

Li, X., Ju, H., Sarah, G., Yan, C., Batchelor, W. D. & Liu, Q. 2017 Spatiotemporal variation of drought characteristics in the Huang-Huai-Hai Plain, China under the climate change scenario. *J. Integr. Agric.* **16**, 2308–2322. https://doi.org/10.1016/S2095-3119(16)61545-9.

Liu, C. L., Zhang, Q., Singh, V. P. & Cui, Y. 2011 Copula-based evaluations of drought variations in Guangdong, South China. *Nat. Hazards* **59**, 1533–1546. https://doi.org/10.1007/s11069-011-9850-4.

Liu, J., Xu, Z., Chen, F., Chen, F. & Zhang, L. 2019 Flood hazard mapping and assessment on the Angkor World Heritage Site, Cambodia. *Remote Sens.* **11**, 1–19. https://doi.org/10.3390/rs11010098.

Lu, G., Wu, H., Xiao, H., He, H. & Wu, Z. 2016 Impact of climate change on drought in the Upstream Yangtze River Region. *Water.* https://doi.org/10.3390/w8120576.

Majidi, A. N., Vojinovic, Z., Alves, A., Weesakul, S., Sanchez, A., Boogaard, F. & Kluck, J. 2019 Planning nature-based solutions for urban flood reduction and thermal comfort enhancement. *Sustainability* **11**. https://doi.org/10.3390/su11226361.

Marcos-Garcia, P., Lopez-Nicolas, A. & Pulido-Velazquez, M. 2017 Combined use of relative drought indices to analyze climate change impact on meteorological and hydrological droughts in a Mediterranean basin. *J. Hydrol.* **554**, 292–305. https://doi.org/10.1016/j.jhydrol.2017.09.028.

Masud, M. B., Khaliq, M. N. & Wheater, H. S. 2015 Analysis of meteorological droughts for the Saskatchewan River Basin using univariate and bivariate approaches. *J. Hydrol.* **522**, 452–466. https://doi.org/10.1016/j.jhydrol.2014.12.058.

Ming, X., Xu, W., Li, Y., Du, J., Liu, B. & Shi, P. 2015 Quantitative multi-hazard risk assessment with vulnerability surface and hazard joint return period. *Stoch. Environ. Res. Risk Assess.* **29**, 35–44. https://doi.org/10.1007/s00477-014-0935-y.

Mishra, A. K. & Singh, V. P. 2010 A review of drought concepts. *J. Hydrol.* **391**, 202–216. https://doi.org/10.1016/j.jhydrol.2010.07.012.

Morita, M. 2011 Quantification of increased flood risk due to global climate change for urban river management planning. *Water Sci. Technol.* **63**, 2967–2974. https://doi.org/10.2166/wst.2011.172.

Nam, W.-H., Hayes, M. J., Svoboda, M. D., Tadesse, T. & Wilhite, D. A. 2015 Drought hazard assessment in the context of climate change for South Korea. *Agric. Water Manage.* **160**, 106–117. https://doi.org/10.1016/j.agwat.2015.06.029.

Nandi, A., Mandal, A., Wilson, M. & Smith, D. 2016 Flood hazard mapping in Jamaica using principal component analysis and logistic regression. *Environ. Earth Sci.* **75**, 1–16. https://doi.org/10.1007/s12665-016-5323-0.

Navarathinam, K., Gusyev, M. A., Hasegawa, A., Magome, J. & Takeuchi, K. 2015 Agricultural flood and drought risk reduction by a proposed multi-purpose dam: A case study of the Malwathoya River Basin, Sri Lanka. In *Proc. - 21st Int. Congr. Model. Simulation, MODSIM 2015.* pp. 1600–1606. https://doi.org/10.13140/RG.2.1.3620.7126.

Nawai, J., Gusyev, M. A., Hasegawa, A. & Takeuchi, K. 2015 Flood and drought assessment with dam infrastructure: A case study of the Ba River basin, Fiji. In *Proc. - 21st Int. Congr. Model. Simulation, MODSIM 2015.* pp. 1607–1613. https://doi.org/10.13140/RG.2.1.2572.1361.

Nelson, R. B. 2006 *An Introduction to Copulas.* Springer, New York.

Nigusse, A. G. & Adhanom, O. G. 2019 Flood hazard and flood risk vulnerability mapping using Geo-Spatial and MCDA around Adigrat, Tigray Region, Northern Ethiopia. *Momona Ethiopian J. Sci.* **11**, 90. https://doi.org/10.4314/mejs.v11i1.6.

Ohba, M. & Sugimoto, S. 2019 Differences in climate change impacts between weather patterns: Possible effects on spatial heterogeneous changes in future extreme rainfall. *Clim. Dyn.* **52**, 4177–4191. https://doi.org/10.1007/s00382-018-4374-1.

O'Neill, B. C., Kriegler, E., Ebi, K. L., Kemp-Benedict, E., Riahi, K., Rothman, D. S., van Ruijven, B. J., van Vuuren, D. P., Birkmann, J., Kok, K., Levy, M. & Solecki, W. 2017 The roads ahead: Narratives for shared socioeconomic pathways describing world futures in the 21st century. *Glob. Environ. Change* **42**, 169–180. https://doi.org/10.1016/j.gloenvcha.2015.01.004.

Ouma, Y. O. & Tateishi, R. 2014 Urban flood vulnerability and risk mapping using integrated multi-parametric AHP and GIS: Methodological overview and case study assessment. *Water (Switzerland)* **6**, 1515–1545. https://doi.org/10.3390/w6061515.

Ozkan, S. P. & Tarhan, C. 2016 Detection of flood hazard in urban areas using GIS: Izmir case. *Procedia Technol.* **22**, 373–381. https://doi.org/10.1016/j.protcy.2016.01.026.

Ozturk, D. & Batuk, F. 2011 Implementation of GIS-based multicriteria decision analysis with VB in ArcGIS. *Int. J. Inf. Technol. Decis. Making* **10**, 1023–1042. https://doi.org/10.1142/S0219622011004695.

Pandey, S., Bhandari, H. & Hardy, B. 2007 *Economic Costs of Drought and Rice Farmers' Coping Mechanisms: A Cross-Country Comparative Analysis.* International Rice Research Institute, Los Baños, Philippines, p. 203.

Paquette, J. & Lowry, J. 2012 Flood hazard modelling and risk assessment in the Nadi River Basin, Fiji, using GIS and MCDA. *South Pacific J. Nat. Appl. Sci.* **30**, 33. https://doi.org/10.1071/sp12003.

Penny, J., Djordjević, S. & Chen, A. S. 2021 Using public participation within land use change scenarios for analysing environmental and socioeconomic drivers. *Environ. Res. Lett.* **17**. https://doi.org/10.1088/1748-9326/ac4764.

Penny, J., Alves, P. B. R., De-silva, Y., Chen, A. S., Djordjevic, S., Shrestha, S. & Babel, M. 2023 Uncorrected proof analysis of potential nature-based solutions for the Mun River Basin, Thailand. *Uncorrected Proof*, 1–19. https://doi.org/10.2166/wst.2023.050.

Peterson, T. C. 2005 Climate change indices. *WMO Bull.* **54** (2), 83–86.

Prabnakorn, S. 2020 *Integrated Flood and Drought Mitigation Measures and Strategies.* https://doi.org/10.1201/9781003024033.

Prabnakorn, S., Maskey, S., Suryadi, F. X. & de Fraiture, C. 2016 Climate and Drought Trends and their relationships with rice production in the Mun river basin, Thailand. In: *2nd World Irrigation Forum.* 6–8 November 2016, Chiang Mai, Thailand.

Prabnakorn, S., Suryadi, F. X., Chongwilaikasem, J. & de Fraiture, C. 2019 Development of an integrated flood hazard assessment model for a complex river system: A case study of the Mun River Basin, Thailand. *Model. Earth Syst. Environ.* **5**, 1265–1281. https://doi.org/10.1007/s40808-019-00634-7.

Prabnakorn, S., Ruangpan, L., Tangdamrongsub, N., Suryadi, F. X. & de Fraiture, C. 2021 Improving flood and drought management in agricultural river basins: An application to the Mun River Basin in Thailand. *Water Policy* **23**, 1153–1169. https://doi.org/10.2166/wp.2021.011.

Rahmati, O., Zeinivand, H. & Besharat, M. 2016 Flood hazard zoning in Yasooj region, Iran, using GIS and multi-criteria decision analysis. *Geomatics Nat. Hazards Risk* **7**, 1000–1017. https://doi.org/10.1080/19475705.2015.1045043.

Rudra, R. P., Dickinson, W. T., Ahmed, S. I., Patel, P., Zhou, J., Gharabaghi, B. & Khan, A. A. 2015 Changes in rainfall extremes in Ontario. *Int. J. Environ. Res.* **9**, 1117–1126. https://doi.org/10.22059/ijer.2015.1000.

Samanta, S., Koloa, C., Pal, D. K. & Palsamanta, B. 2016 Flood risk analysis in lower part of Markham river based on multi-criteria decision approach (MCDA). *Hydrology* **3**, 1–13. https://doi.org/10.3390/hydrology3030029.

Samu, R. & Akıntuğ, B. 2020 Pre-disaster planning and preparedness: Drought and flood forecasting and analysis in Zimbabwe. *Water SA* **46**, 448–457. https://doi.org/10.17159/wsa/2020.v46.i3.8655.

Schipper, E. L. F. 2020 Maladaptation: When adaptation to climate change goes very wrong. *One Earth* **3**, 409–414. https://doi.org/10.1016/j.oneear.2020.09.014.

Shadmehri Toosi, A., Calbimonte, G. H., Nouri, H. & Alaghmand, S. 2019 River basin-scale flood hazard assessment using modified multi-criteria decision analysis approach: A case study. *J. Hydrol.* **574**, 660–671.

Shadmehri Toosi, A., Doulabian, S., Ghasemi Tousi, E., Calbimonte, G. H. & Alaghmand, S. 2020 Large-scale flood hazard assessment under climate change: A case study. *Ecol. Eng.* **147**, 105765. https://doi.org/10.1016/j.ecoleng.2020.105765.

Shah, S. M. H., Mustaffa, Z., Teo, F. Y., Imam, M. A. H., Yusof, K. W. & Al-Qadami, E. H. H. 2020 A review of the flood hazard and risk management in the South Asian Region, particularly Pakistan. *Sci. Afr.* **10**, e00651. https://doi.org/10.1016/j.sciaf.2020.e00651.

Shao, W. & Kam, J. 2020 Retrospective and prospective evaluations of drought and flood. *Sci. Total Environ.* **748**. https://doi.org/10.1016/j.scitotenv.2020.141155.

Shiau, J. T. 2006 Fitting drought duration and severity with two-dimensional copulas. *Water Resour. Manage.* **20**, 795–815. https://doi.org/10.1007/s11269-005-9008-9.

Singhrattna, N., Babel, M. S. & Perret, S. R. 2012 Hydroclimate variability and long-lead forecasting of rainfall over Thailand by large-scale atmospheric variables. *Hydrol. Sci. J.* **57**, 26–41. https://doi.org/10.1080/02626667.2011.633916.

Singkran, N. 2017 Flood risk management in Thailand: Shifting from a passive to a progressive paradigm. *Int. J. Disaster Risk Reduct.* **25**, 92–100. https://doi.org/10.1016/j.ijdrr.2017.08.003.

Sklar, A. 1959 *Fonctions de répartition à n dimensions et leurs marges*. Publication of the Institute of Statistics, University Paris, Paris, Vol. 8, pp. 229–231.

Stagge, J. H., Tallaksen, L. M., Gudmundsson, L., Van Loon, A. F. & Stahl, K. 2015 Candidate distributions for climatological drought indices (SPI and SPEI). *Int. J. Climatol.* **35**, 4027–4040. https://doi.org/10.1002/joc.4267.

Sun, P., Zhang, Q., Yao, R. & Wen, Q. 2019 Hydrological drought regimes of the Huai River. *Water* **11**, 2390. https://doi.org/10.3390/w11112390.

Tabari, H., Hosseinzadehtalaei, P., Thiery, W. & Willems, P. 2021 Amplified drought and flood risk under future socioeconomic and climatic change. *Earth's Futur.* **9**, 1–24. https://doi.org/10.1029/2021EF002295.

Tanavud, C., Yongchalermchai, C., Bennui, A. & Densreeserekul, O. 2004 Assessment of flood risk in Hat Yai Municipality, Southern Thailand, using GIS. *J. Nat. Disaster Sci.* **26**, 1–14. https://doi.org/10.2328/jnds.26.1.

Tang, Z., Zhang, H., Yi, S. & Xiao, Y. 2018 Assessment of flood susceptible areas using spatially explicit, probabilistic multi-criteria decision analysis. *J. Hydrol.* **558**, 144–158. https://doi.org/10.1016/j.jhydrol.2018.01.033.

Vavatsikos, A. P., Demesouka, O. E. & Anagnostopoulos, K. P. 2019 GIS-based suitability analysis using fuzzy PROMETHEE. *J. Environ. Plan. Manage.* **63**, 604–628. https://doi.org/10.1080/09640568.2019.1599830.

Vicente-Serrano, S. M., Beguería, S. & López-Moreno, J. I. 2010 A multiscalar drought index sensitive to global warming: The standardized precipitation evapotranspiration index. *J. Clim.* **23**, 1696–1718. https://doi.org/10.1175/2009JCLI2909.1.

Vojinovic, Z., Hammond, M., Golub, D., Hirunsalee, S., Weesakul, S., Meesuk, V., Medina, N., Sanchez, A., Kumara, S. & Abbott, M. 2016 Holistic approach to flood risk assessment in areas with cultural heritage: A practical application in Ayutthaya, Thailand. *Nat. Hazards* **81**, 589–616. https://doi.org/10.1007/s11069-015-2098-7.

Vojinovic, Z., Alves, A., Gómez, J. P., Weesakul, S., Keerakamolchai, W., Meesuk, V. & Sanchez, A. 2021 Effectiveness of small- and large-scale nature-based solutions for flood mitigation: The case of Ayutthaya, Thailand. *Sci. Total Environ.* **789**, 147725. https://doi.org/10.1016/j.scitotenv.2021.147725.

Wichitarapongsakun, P., Sarin, C., Klomjek, P. & Chuenchooklin, S. 2016 Rainfall prediction and meteorological drought analysis in the Sakae Krang River basin of Thailand. *Agric. Nat. Resour.* **50**, 490–498. https://doi.org/10.1016/j.anres.2016.05.003.

WMO. 2018 *WMO Statement on the Status of the Global Climate in 2017*. World Meteorological Organization, 2017. WMO_1108_EN_web_000.pdf.WMO statement on the status of the global climate in 2017. World Meteorological Organization.

Yang, W., Zhang, L. & Gao, Y. 2023 Drought and flood risk assessment for rainfed agriculture based on Copula-Bayesian conditional probabilities. *Ecol. Indic.* **146**, 109812. https://doi.org/10.1016/j.ecolind.2022.109812.

Zargar, A., Sadiq, R., Naser, B. & Khan, F. I. 2011 A review of drought indices. *Environ. Rev.* **19**, 333–349. https://doi.org/10.1139/a11-013.

Zhang, Q., Gu, X., Singh, V. P., Kong, D. & Chen, X. 2015 Spatiotemporal behavior of floods and droughts and their impacts on agriculture in China. *Glob. Planet. Change* **131**, 63–72. https://doi.org/10.1016/j.gloplacha.2015.05.007.

Zhao, T. & Dai, A. 2017 Uncertainties in historical changes and future projections of drought. Part II: Model-simulated historical and future drought changes. *Clim. Change* **144**, 535–548. https://doi.org/10.1007/s10584-016-1742-x.

Zhu, J. T. 2013 Impact of climate change on extreme rainfall across the United States. *J. Hydrol. Eng.* **18**, 1301–1309. https://doi.org/10.1061/(ASCE)HE.1943-5584.0000725.